arXiv:1608.02212v1 [cond-mat.soft] 7 Aug 2016

Disordered Hyperuniform Heterogeneous Materials

Salvatore Torquato[1,2,3,4]

[1] Department of Chemistry, Princeton University, Princeton, NJ 08544, USA

[2] Department of Physics, Princeton University, Princeton, NJ 08544, USA

[3] Princeton Institute for the Science and Technology of Materials, Princeton, NJ 08544, USA

[4] Program in Applied and Computational Mathematics, Princeton University, Princeton, NJ 08544, USA

Corresponding author contact information:

Salvatore Torquato
Tel.: 609-258-3341
Fax: 609-258-6746
E-mail: torquato@princeton.edu

Short title: Disordered Hyperuniform Heterogeneous Materials

Abstract.

Disordered hyperuniform many-body systems are distinguishable states of matter that lie between a crystal and liquid: they are like perfect crystals in the way they suppress large-scale density fluctuations and yet are like liquids or glasses in that they are statistically isotropic with no Bragg peaks. These systems play a vital role in a number of fundamental and applied problems: glass formation, jamming, rigidity, photonic and electronic band structure, localization of waves and excitations, self-organization, fluid dynamics, quantum systems, and pure mathematics. Much of what we know theoretically about disordered hyperuniform states of matter involves many-particle systems. In this paper, we derive new rigorous criteria that disordered hyperuniform two-phase heterogeneous materials must obey and explore their consequences. Two-phase heterogeneous media are ubiquitous; examples include composites and porous media, biological media, foams, polymer blends, granular media, cellular solids, and colloids. We begin by obtaining some results that apply to hyperuniform two-phase media in which one phase is a sphere packing in d-dimensional Euclidean space $\mathbb{R}^d$. Among other results, we rigorously establish the requirements for packings of spheres of different sizes to be "multihyperuniform." We then consider hyperuniformity for general two-phase media in $\mathbb{R}^d$. Here we apply realizability conditions for an autocovariance function and its associated spectral density of a two-phase medium, and then incorporate hyperuniformity as a constraint in order to derive new conditions. We show that some functional forms can immediately be eliminated from consideration and identify other forms that are allowable. Specific examples and counterexamples are described. Contact is made with well-known microstructural models (e.g., overlapping spheres and checkerboards) as well as irregular phase-separation and Turing-type patterns. We also ascertain a family of autocovariance functions (or spectral densities) that are realizable by disordered hyperuniform two-phase media in any space dimension, and present select explicit constructions of realizations. These studies provide insight into the nature of disordered hyperuniformity in the context of heterogeneous materials and have implications for the design of such novel amorphous materials.

PACS numbers: 05.20.-y,05.40.-a,61.20.Gy,61.50.Ah

Keywords: hyperuniformity, fluctuations, heterogeneous media, disordered materials

1. Introduction

The unusual suppression of density fluctuations at large length scales is central to the hyperuniformity concept, whose broad importance for condensed matter physics and materials science was brought to the fore only about a decade ago in a study that focused on fundamental theoretical aspects, including how it provides a unified means to classify and categorize crystals, quasicrystals and special disordered point configurations [1]. Moreover, it was shown that the hyperuniform many-particle systems are poised at a unique type of critical point in which (normalized) large-scale density fluctuations vanish such that the direct correlation function of the Ornstein-Zernike relation is long-ranged [1]. This is to be contrasted with a standard thermal critical point in which large-scale density fluctuations are infinitely large and the total correlation function (not the direct correlation function) is long-ranged [2, 3, 4, 5].

Roughly speaking, a hyperuniform (or superhomoegeneous [6]) many-particle system in d-dimensional Euclidean space $\mathbb{R}^d$ is one in which (normalized) density fluctuations are completely suppressed at very large length scales, implying that the structure factor $S(\mathbf{k})$ tends to zero as the wavenumber $k \equiv |\mathbf{k}|$ tends to zero, i.e.,

$$\lim_{|\mathbf{k}|\to 0} S(\mathbf{k}) = 0. \tag{1}$$

Equivalently, it is one in which the number variance of particles within a spherical observation window of radius R, denoted by $\sigma_{_N}^2(R)$, grows more slowly than the window volume (R^d) in the large-R limit. Typical disordered systems, such as liquids and structural glasses, have the standard volume scaling, that is, $\sigma_{_N}^2(R) \sim R^d$. By contrast, all perfect crystals and quasicrystals are hyperuniform with the surface-area scaling $\sigma_{_N}^2(R) \sim R^{d-1}$. Surprisingly, there are a special class of disordered particle configurations, such as the one shown in the right panel of Fig. 1, that have the same asymptotic behavior as crystals. There are scalings for the number variance other than surface-area growth. When the structure factor goes to zero in the limit $|\mathbf{k}| \to 0$ with the power-law form

$$S(\mathbf{k}) \sim |\mathbf{k}|^{\alpha}, \tag{2}$$

where $\alpha > 0$, the number variance has the following large-R asymptotic scaling [1, 7, 8]:

$$\sigma_{_N}^2(R) \sim \begin{cases} R^{d-1}, & \alpha > 1, \\ R^{d-1}\ln R, & \alpha = 1 \\ R^{d-\alpha}, & 0 < \alpha < 1 \end{cases} \qquad (R \to \infty). \tag{3}$$

Disordered hyperuniform systems can be regarded to be exotic states of matter that lie between a crystal and liquid: they are like perfect crystals in the way they suppress large-scale density fluctuations and yet are like liquids or glasses in that they are statistically isotropic with no Bragg peaks. In this sense, they can have a *hidden order* (see Fig. 1 for a vivid example) and appear to be endowed with novel physical properties, as described below.

We knew of only a few examples of *disordered* hyperuniform systems about a decade ago [1, 10, 6, 11]. The importance of the hyperuniformity concept in the context of condensed matter started to become apparent when it was shown that classical many-particle systems with certain long-ranged pair potentials could counterintuitively freeze into disordered hyperuniform states at absolute zero with singular scattering patterns, such as the one shown in the right panel of Fig. 2

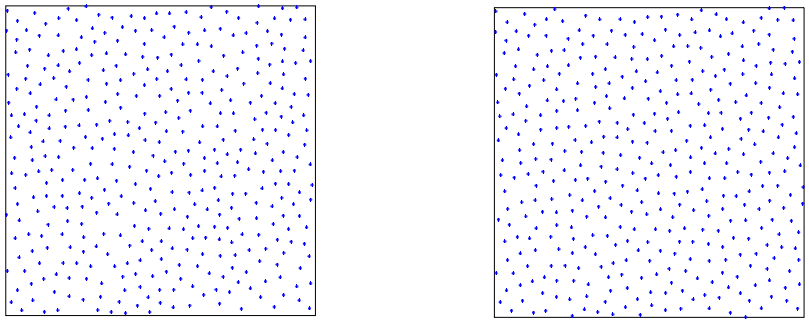

Figure 1. A disordered non-hyperuniform many-particle configuration (left) and a disordered hyperuniform many-particle configuration (right) [9]. The latter is arrived at by very tiny collective displacements of the particles on the left. These two examples show that it can be very difficult to detect hyperuniformity by eye, and yet their large-scale structural properties are dramatically different.

[12, 13]. This exotic situation runs counter to our everyday experience where we expect liquids to freeze into crystal structures (like ice). Mapping such configurations of particles to network structures, what was previously thought to be impossible became possible, namely, the first disordered dielectric networks to have large isotropic photonic band gaps comparable in size to photonic crystals [14]. We now know that these exotic states of matter can exist as both *equilibrium* and *nonequilibrium* phases across space dimensions, including maximally random jammed particle packings [15, 16, 17], jammed athermal granular media [18], jammed thermal colloidal packings [19, 20], dynamical processes in ultracold atoms [21], driven nonequilibrium systems [22, 23, 24, 25, 26, 27], avian photoreceptor patterns [28], geometry of neuronal tracts [29], certain quantum ground states (both fermionic and bosonic) [30, 31], classical disordered (noncrystalline) ground states [9, 12, 13, 32, 33]. A variety of groups have recently fabricated disordered hyperuniform materials at the micro- and nano-scales for various photonic applications [34, 35, 36], surface-enhanced Raman spectroscopy [37], the realization of a terahertz quantum cascade laser [38] and self-assembly of diblock copolymers [39]. Moreover, a computational study revealed that the electronic bandgap of amorphous silicon widens as it tends toward a hyperuniform state [40]. Recent X-ray scattering measurements indicate that amorphous-silicon samples can be made to be nearly hyperuniform [41]. Finally, we note that the hyperuniformity concept has suggested new correlation functions from which one can extract relevant growing length scales as a function of temperature as a liquid is supercooled below its glass transition temperature [42], a problem of intense interest in the glass physics community [43, 44, 45, 46, 47, 48].

The hyperuniformity concept was generalized to the case of two-phase heterogeneous materials [7], which are ubiquitous; examples include composites and porous media, biological media, foams, polymer blends, granular media, cellular solids and colloids [49, 50]. Here the phase volume fraction fluctuates within a finite-sized spherical window of radius R (see Fig. 3) and hence can be characterized by the volume-fraction variance $\sigma_v^2(R)$. For typical disordered two-phase media, the variance $\sigma_v^2(R)$ for large R goes to zero like R^{-d}. However, for hyperuniform disordered two-

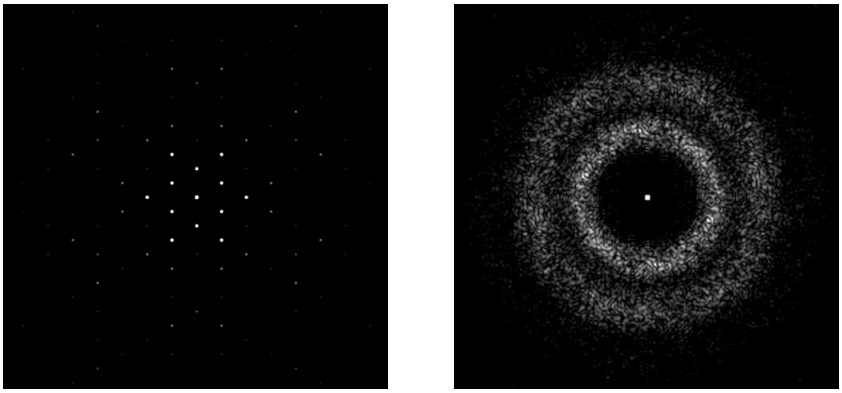

Figure 2. Left: Scattering pattern for a crystal. Right: Scattering pattern for a disordered "stealthy" hyperuniform material (defined in Sec. 2.1). Notice that apart from forward scattering, there is a circle around the origin in which there is no scattering, a highly exotic situation for an amorphous state of matter.

phase media, $\sigma_V^2(R)$ goes to zero asymptotically more rapidly than the inverse of the window volume, i.e., faster than R^{-d}, which is equivalent to the following condition on the spectral density (defined in Sec. 2):

$$\lim_{|\mathbf{k}|\to 0} \tilde{\chi}_V(\mathbf{k}) = 0. \tag{4}$$

As in the case of hyperuniform point configurations [1, 7, 8], three different scaling regimes when the spectral density goes to zero with the power-law form $\tilde{\chi}_V(\mathbf{k}) \sim |\mathbf{k}|^\alpha$:

$$\sigma_V^2(R) \sim \begin{cases} R^{-(d+1)}, & \alpha > 1 \\ R^{-(d+1)} \ln R, & \alpha = 1 \\ R^{-(d+\alpha)}, & 0 < \alpha < 1 \end{cases} \qquad (R \to \infty), \tag{5}$$

where the exponent α is a positive constant.

Much of our recent theoretical understanding of hyperuniform states of matter is based on many-particle systems. The purpose of this paper is to delve more deeply into theoretical foundations of disordered hyperuniform two-phase media by establishing new rigorous criteria that such systems must obey and exploring their consequences.

In Sec. 2, we provide necessary mathematical definitions and background. In Sec. 3, we derive some results concerning hyperuniformity of two-phase systems in $\mathbb{R}^d$ in which one phase is a sphere packing and the spheres generally have different sizes. We determine the necessary and sufficient conditions for a sphere packing to be stealthy and hyperuniform, and prove that when each subpacking associated with each component is hyperuniform, the entire packing is hyperuniform: a property called "multihyperuniformity" [28]. In Sec. 4, we consider hyperuniformity for general two-phase media that lie outside the special class that are derived from sphere packings in d-dimensional Euclidean space $\mathbb{R}^d$. Here we apply realizability conditions for an autocovariance function and its associated spectral density of a two-phase medium, and then incorporate hyperuniformity as a constraint in order to derive new conditions. We demonstrate that some functional forms can immediately be eliminated from consideration, but also identify other forms that are allowable. Specific examples and counterexamples are described, including remarks about well-known microstructural models (e.g., overlapping spheres and checkerboards) as well

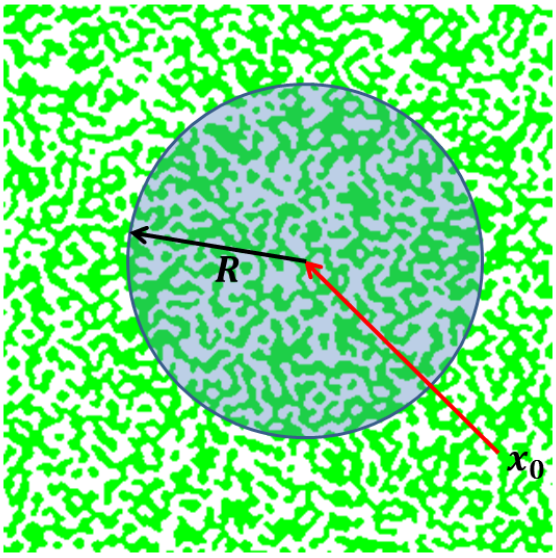

Figure 3. A schematic indicating a circular observation window of radius R that is centered at position $\mathbf{x_0}$ in a disordered two-phase medium; one phase is depicted as a green region and the other phase as a white region. The phase volume fractions within the window will fluctuate as the window position $\mathbf{x}_0$ is varied.

as irregular phase-separation and Turing-type patterns. We also ascertain a family of autocovariance functions that are realizable by disordered hyperuniform two-phase media in arbitrary space dimensions, In Sec. 5, we close with some concluding remarks.

2. Background

2.1. Point Configurations

Consider statistically homogeneous point configurations in d-dimensional Euclidean space $\mathbb{R}^d$. The standard pair correlation function $g_2(\mathbf{r})$ is proportional to the probability density associated with finding pairs of points separated by the displacement vector $\mathbf{r}$, and is normalized in such a way that it tends to unity in the limit $|\mathbf{r}| \to \infty$ in the absence of long-range order. The *total correlation function* $h(\mathbf{r})$ is defined as

$$h(\mathbf{r}) = g_2(\mathbf{r}) - 1. \tag{6}$$

The nonnegative structure factor $S(\mathbf{k})$, which is proportional to the scattering intensity, is trivially related to the Fourier transform of $h(\mathbf{r})$:

$$S(\mathbf{k}) = 1 + \rho\tilde{h}(\mathbf{k}). \tag{7}$$

Appendix A provides definitions of the d-dimensional Fourier transforms that we use in this paper.

The local number variance $\sigma_N^2(R)$ is determined entirely by pair correlations [1]:

$$\sigma_N^2(R) = \rho v_1(R)\Big[1 + \rho \int_{\mathbb{R}^d} h(\mathbf{r})\alpha(r;R)d\mathbf{r}\Big]$$
$$= \rho v_1(R)\Big[\frac{1}{(2\pi)^d}\int_{\mathbb{R}^d} S(\mathbf{k})\tilde{\alpha}(k;R)d\mathbf{k}\Big], \tag{8}$$

where $v_1(R) = \pi^{d/2}R^d/\Gamma(1+d/2)$ is the d-dimensional volume of a spherical window, $\alpha(r;R)$ is the intersection volume of two identical hyperspheres of radius R (scaled by the volume of a sphere) whose centers are separated by a distance r, which is known analytically in any space dimension [1, 51], and $\tilde{\alpha}(k;R)$ is its Fourier transform, which is nonnegative and explicitly given by

$$\tilde{\alpha}(k;R) = 2^d\pi^{d/2}\Gamma(1+d/2)\frac{[J_{d/2}(kR)]^2}{k^d}. \tag{9}$$

Here $J_\nu(x)$ is the Bessel function of order ν.

As mentioned earlier, the hyperuniformity property for point configurations is specified by the structure-factor condition (1). *Stealthy* configurations are those in which the structure factor is exactly zero for a subset of wave vectors, meaning that they completely suppress single scattering of incident radiation for these wave vectors [13]. Stealthy *hyperuniform* patterns [9, 12, 13] are a subclass of hyperuniform systems in which the structure factor is zero for a range of wave vectors around the origin, i.e.,

$$S(\mathbf{k}) = 0 \qquad \text{for } 0 \le |\mathbf{k}| \le K, \tag{10}$$

where K is some positive number. An example of a stealthy disordered scattering pattern is shown in the right panel of Fig. 2.

2.2. Two-Phase Media

A two-phase random medium is a domain of space $\mathcal{V} \subseteq \mathbb{R}^d$ of volume V that is partitioned into two disjoint regions that make up $\mathcal{V}$: a phase 1 region $\mathcal{V}_1$ of volume fraction ϕ_1 and a phase 2 region $\mathcal{V}_2$ of volume fraction ϕ_2 [49].

2.2.1. Two-Point Statistics The phase indicator function $\mathcal{I}^{(i)}(\mathbf{x})$ for a given realization is defined as

$$\mathcal{I}^{(i)}(\mathbf{x}) = \begin{cases} 1, & \mathbf{x} \in \mathcal{V}_i, \\ 0, & \mathbf{x} \notin \mathcal{V}_i, \end{cases} \tag{11}$$

The one-point correlation function $S_1^{(i)}(\mathbf{x}) = \langle \mathcal{I}^{(i)}(\mathbf{x})\rangle$ (where angular brackets indicate an ensemble average) is generally dependent on the position $\mathbf{x}$, but is a constant for statistically homogeneous media, namely, the phase volume fraction, i.e.,

$$\phi_i = \langle \mathcal{I}^{(i)}(\mathbf{x})\rangle, \tag{12}$$

such that $\phi_1 + \phi_2 = 1$. The two-point correlation function is defined as $S_2^{(i)}(\mathbf{x}_1, \mathbf{x}_2) = \big\langle \mathcal{I}^{(i)}(\mathbf{x}_1)\mathcal{I}^{(i)}(\mathbf{x}_2)\big\rangle$. This function is the probability of finding two points at positions $\mathbf{x}_1$ and $\mathbf{x}_2$ in phase i. For statistically homogeneous media, the two-point correlation function will only depend on the relative displacement vector $\mathbf{r} \equiv \mathbf{x}_2 - \mathbf{x}_1$ and hence $S_2^{(i)}(\mathbf{x}_1, \mathbf{x}_2) = S_2^{(i)}(\mathbf{r})$. The autocovariance function $\chi_{_V}(\mathbf{r})$ associated with the random variable $\mathcal{I}^{(i)}(\mathbf{x})$ for phase 1 is equal to that for phase 2, i.e.,

$$\chi_{_V}(\mathbf{r}) \equiv S_2^{(1)}(\mathbf{r}) - {\phi_1}^2 = S_2^{(2)}(\mathbf{r}) - {\phi_2}^2. \tag{13}$$

At the extreme limits of its argument, χ_V has the following asymptotic behavior

$$\chi_V(\mathbf{r}=0) = \phi_1\phi_2, \qquad \lim_{|\mathbf{r}|\to\infty} \chi_V(\mathbf{r}) = 0, \tag{14}$$

the latter limit applying when the medium possesses no long-range order. If the medium is statistically homogeneous and isotropic, then the autocovariance function $\chi_V(\mathbf{r})$ depends only on the magnitude of its argument $r = |\mathbf{r}|$, and hence is a radial function. In such instances, its slope at the origin is directly related to the *specific surface* s (interface area per unit volume); specifically, we have in any space dimension d, the asymptotic form [49],

$$\chi_V(\mathbf{r}) = \phi_1\phi_2 - \beta(d)s\,|\mathbf{r}| + \mathcal{O}(|\mathbf{r}|^2), \tag{15}$$

where

$$\beta(d) = \frac{\Gamma(d/2)}{2\sqrt{\pi}\Gamma((d+1)/2)}. \tag{16}$$

The nonnegative spectral density $\tilde{\chi}_V(\mathbf{k})$, which can be obtained from scattering experiments [52, 53], is the Fourier transform of $\chi_V(\mathbf{r})$, i.e.,

$$\tilde{\chi}_V(\mathbf{k}) = \int_{\mathbb{R}^d} \chi_V(\mathbf{r}) e^{-i\mathbf{k}\cdot\mathbf{r}} \mathrm{d}\mathbf{r} \geq 0, \qquad \text{for all } \mathbf{k}. \tag{17}$$

For isotropic media, the spectral density only depends on $k = |\mathbf{k}|$ and, as a consequence of (15), its decay in the large-k limit is controlled by the exact following power-law form:

$$\tilde{\chi}_V(\mathbf{k}) \sim \frac{\gamma(d)\, s}{k^{d+1}}, \qquad k \to \infty, \tag{18}$$

where

$$\gamma(d) = 2^d\, \pi^{(d-1)/2}\, \Gamma((d+1)/2) \tag{19}$$

is a d-dimensional constant.

The higher-order correlation functions $S_3, S_4, \ldots$ [49, 54, 55] will not be considered here, but we note that they arise in rigorous bounds and exact expressions for effective transport [49, 56, 57, 58, 59, 60, 61, 62, 63], elastic [49, 58, 60, 61, 64] and electromagnetic [65] properties of two-phase media.

2.2.2. Realizability Conditions on Autocovariance Functions of Two-Phase Media A necessary and sufficient condition for the existence of a scalar autocovariance function of a stochastically continuous homogeneous process is that its spectral function must be a nonnegative bounded measure [49, 66]. However, it is known that for a two-phase system characterized by the phase indicator function (11), the nonnegativity property of the spectral function [cf. (17)] is a necessary but generally not sufficient condition for the existence of an autocovariance function $\chi_V(\mathbf{r})$ corresponding to a two-phase medium [49, 51, 67, 68, 69, 70]. The autocovariance function must also satisfy other conditions, which are most conveniently stated in terms of the scaled autocovariance function $f(\mathbf{r})$, which is defined by

$$f(\mathbf{r}) \equiv \frac{\chi_V(\mathbf{r})}{\phi_1\phi_2}. \tag{20}$$

Comparing this to relation (14), we see that

$$f(\mathbf{r}=0) = 1, \qquad \lim_{|\mathbf{r}|\to\infty} f(\mathbf{r}) = 0. \tag{21}$$

We let $\tilde{f}(\mathbf{k})$ denote the Fourier transform of $f(\mathbf{r})$, implying that

$$\tilde{f}(\mathbf{k}) = \frac{\tilde{\chi}_V(\mathbf{k})}{\phi_1\phi_2} \geq 0 \qquad \text{for all } \mathbf{k}. \tag{22}$$

Among other conditions, the scaled autocovariance function must satisfy the following bounds for all $\mathbf{r}$:

$$-\min\left[\frac{\phi_1}{\phi_2}, \frac{\phi_2}{\phi_1}\right] \leq f(\mathbf{r}) \leq 1. \tag{23}$$

Another necessary condition on $f(\mathbf{r})$ in the case of statistically homogeneous and isotropic media, i.e., when $f(\mathbf{r})$ is dependent only on the distance $r \equiv |\mathbf{r}|$, is that its derivative at $r = 0$ is strictly negative for all $0 < \phi_i < 1$:

$$\left.\frac{\mathrm{d}f}{\mathrm{d}r}\right|_{r=0} < 0, \tag{24}$$

which is consistent with the fact that slope at $r = 0$ is proportional to the negative of the specific surface s [cf. (15)]. Since $f(|\mathbf{r}|)$ is an even function (i.e., $f(\mathbf{r}) = f(-\mathbf{r})$) that is linear in $|\mathbf{r}|$ at the origin, it is nonanalytic at the origin. This is rather a strong restriction because it eliminates any function that is analytic at the origin (which necessarily implies even powers of $|\mathbf{r}|$); for example, it prohibits autocovariance functions of a Gaussian form [e.g., $\exp(-(r/a)^2)$]. For statistically homogeneous media, another condition is the so-called "triangular inequality":

$$f(\mathbf{r}) \geq f(\mathbf{s}) + f(\mathbf{t}) - 1, \tag{25}$$

where $\mathbf{r} = \mathbf{t} - \mathbf{s}$. If the autocovariance function of a statistically homogeneous and isotropic medium is monotonically decreasing, nonnegative and convex (i.e., $\mathrm{d}^2 f/\mathrm{d}^2 r \geq 0$), then it satisfies the triangular inequality (25). The triangular inequality implies several pointwise conditions on $f(\mathbf{r})$. For example, for statistically homogeneous and isotropic media, it implies the condition (24) and convexity at the origin:

$$\left.\frac{\mathrm{d}^2 f}{\mathrm{d}r^2}\right|_{r=0} \geq 0. \tag{26}$$

The triangular inequality is actually a special case of the following more general condition:

$$\sum_{i=1}^{m}\sum_{j=1}^{m} \varepsilon_i \varepsilon_j f(\mathbf{r}_i - \mathbf{r}_j) \geq 1, \tag{27}$$

where $\varepsilon_i = \pm 1$ ($i = 1, ..., m$ and m is odd). Note that by choosing $m = 3$; $\varepsilon_1\varepsilon_2 = 1$, $\varepsilon_1\varepsilon_3 = \varepsilon_2\varepsilon_3 = -1$, Eq. (25) can be rediscovered. If $m = 3$; $\varepsilon_1\varepsilon_2 = \varepsilon_1\varepsilon_3 = \varepsilon_2\varepsilon_3 = 1$ are chosen instead, another "triangular inequality" can be obtained, i.e.,

$$f(\mathbf{r}) \geq -f(\mathbf{s}) - f(\mathbf{t}) - 1, \tag{28}$$

where $\mathbf{r} = \mathbf{t} - \mathbf{s}$. Equation (28) was first derived by Quintanilla [69]. Equation (27) is a much stronger necessary condition that implies that there are other necessary conditions beyond those identified thus far. However, Eq. (27) is difficult to check in practice, because it does not have a simple spectral analog.

2.2.3. Local Volume-Fraction Variance and Spectral Density It is known that the volume-fraction variance $\sigma_{_V}^2(R)$ within a d-dimensional spherical window of radius R can be expressed in terms of the autocovariance function $\chi_{_V}(\mathbf{r})$ [71]:

$$\sigma_{_V}^2(R) = \frac{1}{v_1(R)} \int_{\mathbb{R}^d} \chi_{_V}(\mathbf{r}) \alpha(r;R) d\mathbf{r}, \tag{29}$$

where

$$v_1(R) = \frac{\pi^{d/2} R^d}{\Gamma(1+d/2)} \tag{30}$$

is the volume of a d-dimensional sphere of radius R, and $\alpha(r;R)$ is the scaled intersection volume, as defined in Eq. (8). ‡ The alternative Fourier representation of the volume-fraction variance that is dual to the direct-space representation (29) is trivially obtained by applying Parseval's theorem to (29) under the assumption that the spectral density $\tilde{\chi}_{_V}(\mathbf{k})$ [Fourier transform of $\chi_{_V}(\mathbf{r})$] exists:

$$\sigma_{_V}^2(R) = \frac{1}{v_1(R)(2\pi)^d} \int_{\mathbb{R}^d} \tilde{\chi}_{_V}(\mathbf{k}) \tilde{\alpha}(k;R) d\mathbf{k}. \tag{31}$$

Note that the hyperuniformity condition (4) dictates that the direct-space autocovariance function $\chi_{_V}(\mathbf{r})$ exhibits both positive and negative correlations such that its volume integral over all space is exactly zero, i.e.,

$$\int_{\mathbb{R}^d} \chi_{_V}(\mathbf{r}) d\mathbf{r} = 0, \tag{32}$$

which can be thought of as a sum rule. The generalization of the hyperuniformity concept to two-phase systems has been fruitfully applied to characterize a variety of disordered sphere packings [15, 20, 73, 74, 75].

3. Hyperuniform Sphere Packings

Here we collect in one place various known results scattered throughout the literature concerning the autocovariance function $\chi_{_V}(\mathbf{r})$ and spectral density $\tilde{\chi}_{_V}(\mathbf{k})$ for two-phase media in $\mathbb{R}^d$ in which one phase is a sphere packing in order to make some remarks about hyperuniformity and stealthiness. A particle packing is a configuration of nonoverlapping (i.e., hard) particles in $\mathbb{R}^d$. For statistically homogeneous packings of congruent spheres of radius a in $\mathbb{R}^d$ at number density ρ, the two-point probability function $S_2(\mathbf{r})$ of the particle (sphere) phase is known exactly in terms of the pair correlation function [49, 76], yielding the autocovariance function as

$$\begin{aligned} \chi_{_V}(\mathbf{r}) &= \rho\, m(r;a) \otimes m(r;a) + \rho^2 m(r;a) \otimes m(r;a) \otimes h(\mathbf{r}) \\ &= \rho\, v_2^{int}(r;a) + \rho^2 v_2^{int}(r;a) \otimes h(\mathbf{r}), \end{aligned} \tag{33}$$

where

$$m(r;a) = \Theta(a-r) = \begin{cases} 1, & r \le a, \\ 0, & r > a, \end{cases} \tag{34}$$

is the sphere indicator function, and $v_2^{int}(r;a) = v_1(a)\alpha(r;a)$ is the intersection volume of two spherical windows of radius a whose centers are separated by a distance r, where

‡ Note that we have changed the earlier notation for the volume-fraction variance used in Ref. [7] from $\sigma_\tau^2(R)$ to $\sigma_{_V}^2(R)$ to distinguish it from other variance functions that have been introduced elsewhere [72] to describe generalizations of the hyperuniformity concept.

$v_1(a)$ and $\alpha(r;a)$ are defined as in (29), and $\otimes$ denotes the convolution of two functions $F(\mathbf{r})$ and $G(\mathbf{r})$:

$$F(\mathbf{r}) \otimes G(\mathbf{r}) = \int_{\mathbb{R}^d} F(\mathbf{x})G(\mathbf{r}-\mathbf{x})d\mathbf{x}. \tag{35}$$

Fourier transformation of (33) gives the corresponding spectral density in terms of the structure factor [7, 49, 76]:

$$\begin{aligned}\tilde{\chi}_{_V}(\mathbf{k}) &= \rho\,\tilde{m}^2(k;a) + \rho^2\tilde{m}^2(k;a)\tilde{h}(\mathbf{k})\\ &= \rho\,\tilde{m}^2(k;a)S(\mathbf{k})\\ &= \phi\tilde{\alpha}(k;a)S(\mathbf{k})\end{aligned} \tag{36}$$

where

$$\tilde{\alpha}(k;a) = \frac{1}{v_1(a)}\tilde{m}^2(k;a) = \frac{1}{v_1(a)}\left(\frac{2\pi a}{k}\right)^d J^2_{d/2}(ka), \tag{37}$$

$$\phi = \rho v_1(a), \tag{38}$$

is the *packing fraction*, defined to be the fraction of space covered by the nonoverlapping spheres, and $v_1(a)$ is the volume of a sphere of radius a defined by (30).

We can bound the volume-fraction variance $\sigma^2_{_V}(R)$ from above in terms of the number variance $\sigma^2_{_N}(R)$ for some fixed R. This is accomplished by substituting the second line of (36) into the integral expression (31), employing the number-variance relation (8) and using the fact that $\tilde{m}(k;a)$ achieves its maximum value of $v_1(a)$ at $k=0$. This leads to the following upper bound:

$$\sigma^2_{_V}(R) \le \left(\frac{a}{R}\right)^{2d}\sigma^2_{_N}(R) \qquad \text{for all } R, \tag{39}$$

In Ref. [7], the same bound was given, but was derived for the large-R asymptotic limit. Bound (39) is in fact valid for any R.

We now show that the hyperuniformity of a sphere packing in terms of volume-fraction fluctuations can only arise if the underlying point configuration (determined by the sphere centers) is itself hyperuniform. Since $\tilde{\alpha}(k;a)$ is analytic at $k=0$, we have that in the limit $k\to 0$,

$$\tilde{\alpha}(k;a) = \frac{\pi^{d/2}R^d}{\Gamma(1+d/2)}\left[1 - \frac{(ka)^2}{d+2} + \mathcal{O}(k^4)\right], \tag{40}$$

Because $\tilde{\alpha}(k;a)$ is a positive well-behaved function in the vicinity of the origin, it immediately follows from expression (36) that if the underlying point process is hyperuniform, as per the structure-factor condition (1), then the spectral density $\tilde{\chi}_{_V}(\mathbf{k})$ inherits the hyperuniformity property (4) only through the structure factor, not $\tilde{\alpha}(k;a)$. The stealthiness property (no scattering at some finite subset of wave vectors) is a bit more subtle. We see from relation (36) that $\tilde{\chi}_{_V}(\mathbf{k})$ is zero at those wave vectors where $S(\mathbf{k})$ is zero as well as at the zeros of the function $\tilde{\alpha}(k;a)$, which is determined by the zeros of the Bessel function $J_{d/2}(ka)$.

To illustrate the utility of these results, we now consider an example where the spectral density as well as the volume-fraction variance can be calculated exactly for a sphere-packing model as density increases up to a maximal value corresponding to hyperuniform state. Specifically, we compute these quantities for sphere packings corresponding to a g_2-invariant process introduced by Torquato and Stillinger [1]. A

g_2-invariant process is one in which a chosen nonnegative form for the pair correlation function g_2 remains invariant over a nonvanishing density range while keeping all other relevant macroscopic variables fixed [77]. The upper limiting "terminal" density is the point above which the nonnegativity condition on the structure factor [cf. (7)] would be violated. Thus, whenever the structure factor attains its minimum value of zero at $\mathbf{k} = 0$ at the terminal or critical density, the system, if realizable, is hyperuniform. In Ref. [1], a variety of hyperuniform g_2-invariant processes in which the number variance $\sigma_{_N}^2(R)$ grows like the window surface area (i.e., R^{d-1}) were exactly studied in arbitrary space dimensions. For our purposes, we employ the "step-function" g_2-invariant process, namely, a $g_2(r)$ that is defined by the unit step function $\Theta(r - D)$, where $D = 2a$ is the sphere diameter. The corresponding structure factor in the density range $0 \le \rho \le \rho_c$ is given by

$$S(k) = 1 - \Gamma(1 + d/2) \left(\frac{2}{kD}\right)^{d/2} \left(\frac{\rho}{\rho_c}\right) J_{d/2}(kD), \tag{41}$$

where $\rho_c = [2^d v_1(D/2)]^{-1}$ is the terminal density at which the packing is hyperuniform [1]. For $\rho < \rho_c$, the packing is not hyperuniform. Substitution of (41) into relation (36) yields the associated spectral density for this model in d dimensions:

$$\tilde{\chi}_{_V}(\mathbf{k}) = \rho \left(\frac{\pi D}{k}\right)^d J_{d/2}^2(kD/2) \left[1 - \Gamma(1 + d/2) \left(\frac{2}{kD}\right)^{d/2} \left(\frac{\rho}{\rho_c}\right) J_{d/2}(kD)\right]. \tag{42}$$

The top panel of Fig. 4 shows the spectral function $\tilde{\chi}_{_V}(k)$ for the aforementioned g_2-invariant packing process in three dimensions at two different densities: one at a non-hyperuniform density $\rho = \rho_c/2$ and the other at the hyperuniform terminal density ρ_c, where $\rho_c = \rho = 3/(4\pi)$, as obtained from (42). As noted above, the degree of hyperuniformity reflected in $\tilde{\chi}_{_V}(k)$ is inherited from the properties of the structure factor. Note that value of the spectral density at the origin for $\rho = \rho_c/2$ would monotonically decrease as the density increases up to the terminal density at which point it is exactly zero. The bottom panel of this figures depicts the associated local volume-fraction variance $\sigma_{_V}^2(R)$ multiplied by R^3 for these two packings, as obtained from relation (31). Observe that because $\sigma_{_V}^2(R)$ for the non-hyperuniform curve decays like R^{-3} for large R, the product $\sigma_{_V}^2(R)R^3$ asymptotes to a constant value. By contrast, the product $\sigma_{_V}^2(R)R^3$ for $\rho = \rho_c$ decays like R^{-1} for large R, as it should for this three-dimensional hyperuniform two-phase system.

The aforementioned results for the pair statistics in both direct and Fourier spaces for identical spheres have been generalized to the case of impenetrable spheres with a continuous or discrete size distribution at overall number density ρ [49, 78]. We collect these results in Appendix B in order and prove there that when each subpacking associated with each component is hyperuniform, the entire packing is hyperuniform, what has been termed *multihyperuniformity* [28]. It is important to note that examining the structure factor $S(\mathbf{k})$ of the point configurations derived from the centers of spheres with a polydispersity in size could lead one to incorrectly conclude that the packings were not hyperuniform. It has been demonstrated [15, 73, 74] that the proper means of investigating hyperuniformity in this case is through a packing's spectral density $\tilde{\chi}_{_V}(\mathbf{k})$. This has also been confirmed in experimental studies of maximally random jammed packings of colloidal spherical particles with a size distribution [20].

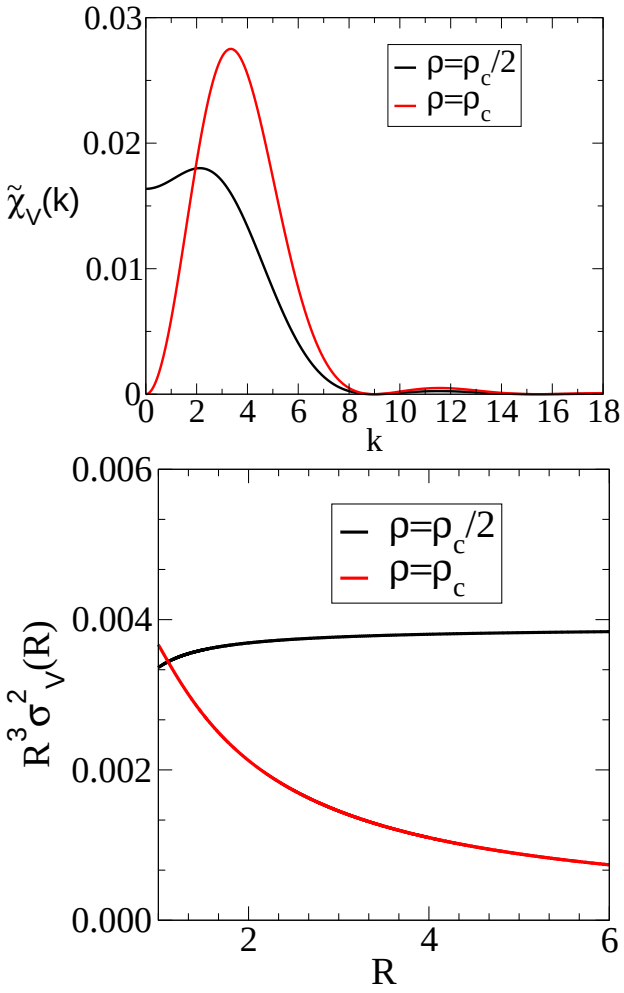

Figure 4. Top panel: A hyperuniform spectral density $\tilde{\chi}_V(k)$ versus wavenumber k for sphere packings corresponding to the step-function g_2-invariant process in three dimensions at two different densities: one at a non-hyperuniform density $\rho = \rho_c/2$ and the other at the hyperuniform terminal density ρ_c, where $\rho_c = \rho = 3/(4\pi)$ [1]. Bottom panel: The corresponding volume-fraction variance $\sigma_V^2(R)$ versus window sphere radius R for the non-hyperuniform and hyperuniform cases. The diameter of a hard sphere is the unit distance that makes all relevant dimensional variables dimensionless.

4. Hyperuniformity Conditions for a General Class of Two-Phase Media

Our interest here is to elucidate our understanding of hyperuniformity in general two-phase media that lie outside the special class that are derived from sphere packings, as per the previous section. This is accomplished by applying the realizability conditions for an autocovariance function of a two-phase medium that is also hyperuniform. We show that some functional forms can immediately be eliminated from consideration and that other forms are allowable. Specific examples and counterexamples are described. We note that it trivially follows from (32) that the scaled autocovariance

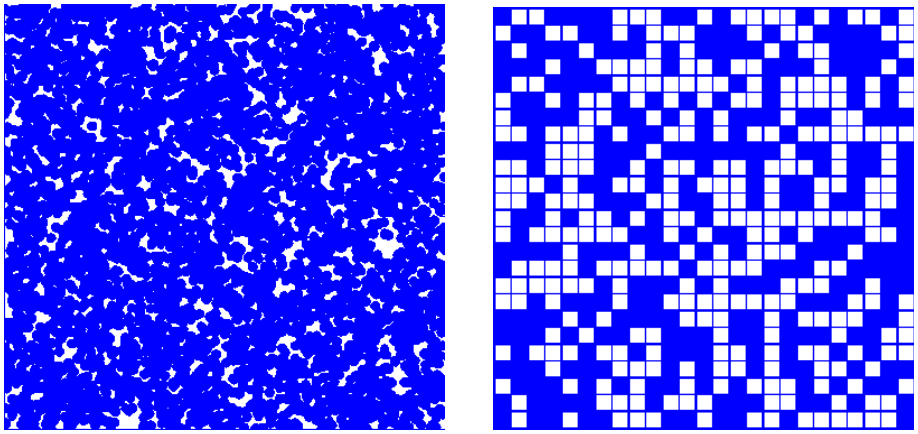

Figure 5. Realizations of overlapping circular disks at $\phi_2 = 0.885$ (left) and of a random checkerboard at $\phi_2 = 0.5$.

$f(\mathbf{r})$ obeys the sum rule

$$\int_{\mathbb{R}^d} f(\mathbf{r}) d\mathbf{r} = 0. \tag{43}$$

When $f(\mathbf{r})$ is a function of the modulus $r = |\mathbf{r}|$, this sum rule reduces to the following one-dimensional integral condition:

$$\int_0^\infty r^{d-1} f(r) dr = 0. \tag{44}$$

4.1. Monotonic Autocovariance Functions

To begin, it is instructive to illustrate the capacity of the sum rule (43) to eliminate an enormous set of two-phase structures from the hyperuniform class. First, we make the simple observation that any two-phase medium with a scaled autocovariance function $f(\mathbf{r})$ that *monotonically decreases* from its maximum value of unity at the origin to its long-range value, such as the well-known overlapping-sphere and symmetric-cell models [79, 49], cannot be hyperuniform at any positive volume fraction, since the sum rule (43) requires that the autocovariance function $\chi_v(\mathbf{r})$ possess both positive and negative values such that its volume integral over all space be zero. The overlapping-sphere model in $\mathbb{R}^d$ consists of the union of spheres that circumscribe the points generated from a Poisson distribution. The symmetric-cell model is derived from a tessellation of space into "cells" with cells being randomly designated as phase 1 and phase 2 with probability ϕ_1 and ϕ_2, respectively. Figure 5 shows two-dimensional realizations of each of these models. We note that while these are idealized models, there are many real two-phase systems (e.g., sandstones and ceramic-metal composites) that have similar monotonic autocovariance functions [49, 80] and hence can be immediately ruled out as hyperuniform structures. Moreover, it is noteworthy that there is a huge class of two-phase systems that exhibit strong positive and negative pair correlations at small pair distances (e.g., equilibrium and nonequilibrium distributions of nonoverlapping particles) that nonetheless are not hyperuniform by virtue of the fact that their autocovariance functions violate the sum rule (43) [81, 76, 49].

4.2. Remarks About Phase-Separation and Turing Patterns

There are a variety of interesting spatial patterns that arise in biological and chemical systems that result from a competition between different pattern instabilities with selected wavelengths. Such phenomena have been theoretically described by, for example, Cahn-Hilliard equations [82] and Swift-Hohenberg equations [83], whose solutions can lead to irregular phase-separation and Turing patterns with a well-defined characteristic wavelength. Thus, it is plausible that binarized (two-phase) patterns obtained by thresholding such scalar fields might be hyperuniform or even stealthy and hyperuniform. An example of a Turing pattern with an irregular labyrinth-like structure [84] is shown in Fig. 6. The distance between adjacent "channels" of the labyrinth-type pattern is a physical display of the wavelength (or wavenumber) that has been selected, which is roughly equal to the mean chord length ℓ_C [49]. Also, depicted in this figure is the autocovariance function $\chi_V(\mathbf{r})$ associated with the thresholded binarized (two-phase) version of the Turing image. This function exhibits strong positive as well as negative correlations at short distances. The top panel of Figure 7 shows the spectral density $\tilde{\chi}_V(\mathbf{k})$ obtained from the thresholded image. Note that it exhibits a well-defined annulus in which scattering intensity is enhanced relative to that in the region outside this annulus, which is radially centered at $k\,\ell_C \approx 7$. The bottom panel of Fig. 7 shows the angular-averaged spectral density from which we conclude that the thresholded Turing pattern is neither stealthy nor hyperuniform.

While this outcome does not mean that thresholded Turing-type patterns can never be hyperuniform, it does lead to the following question: Are there disordered stealthy and hyperuniform two-phase systems with spectral densities in which scattering is concentrated within some relatively thin annulus defined by a small range of wavenumbers away from the origin? To answer this question, we consider the following hypothetical, idealized scaled spectral functions to see if they can fall within this possible stealthy and hyperuniform class:

$$\tilde{f}_A(\mathbf{k}) = c_A(d)\delta(k-K) \tag{45}$$

and

$$\tilde{f}_B(\mathbf{k}) = \begin{cases} c_B(d), & K_1 \le k \le K_2, \\ 0, & \text{otherwise}, \end{cases} \tag{46}$$

where $\delta(k)$ is a radial Dirac delta function is d-dimensional Fourier space, $K_2 > K_1$,

$$c_A(d) = \frac{2^{d-1}\,\pi^{d/2}\,\Gamma(d/2)}{K^{d-1}} \tag{47}$$

and

$$c_B(d) = (2\pi)^{d/2}\,\Gamma(d/2+1)\frac{(K_1^d - K_2^d)}{K_1^d K_2^d}. \tag{48}$$

Using the results of Appendix A, the corresponding hypothetical scaled autocovariance function, which obeys the exact limiting conditions (21), are given by

$$f_A(\mathbf{r}) = \left(\frac{2}{Kr}\right)^{d/2-1} \Gamma(d/2)\,J_{d/2-1}(Kr), \tag{49}$$

and

$$f_B(\mathbf{r}) = F(r;K_2) - F(r;K_1), \tag{50}$$

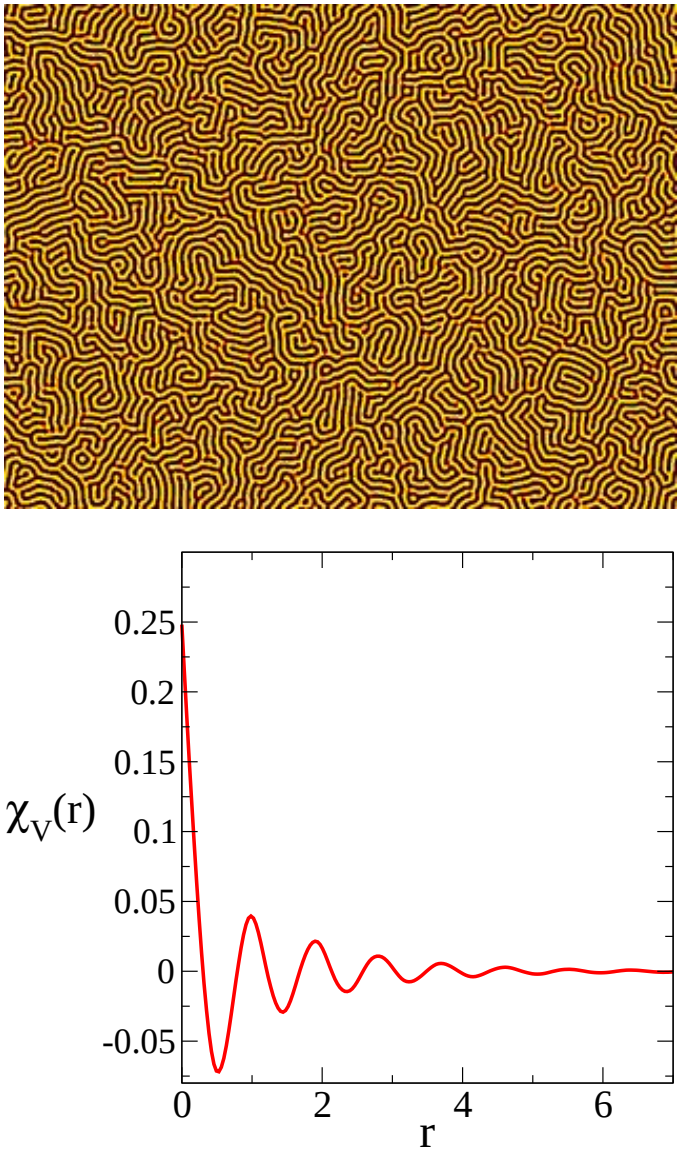

Figure 6. Top left panel: Image of a Turing pattern with a labyrinth-like structure [84]. Bottom panel: The autocovariance function $\chi_V(\mathbf{r})$ associated with the thresholded version of the Turing image (with $\phi_1 \approx \phi_2 = 1/2$), showing strong short-range order, including anti-correlations (negative values). The unit of distance is the mean chord length of the "yellow" phase [49], which is roughly equal to the characteristic width of the "channels."

.

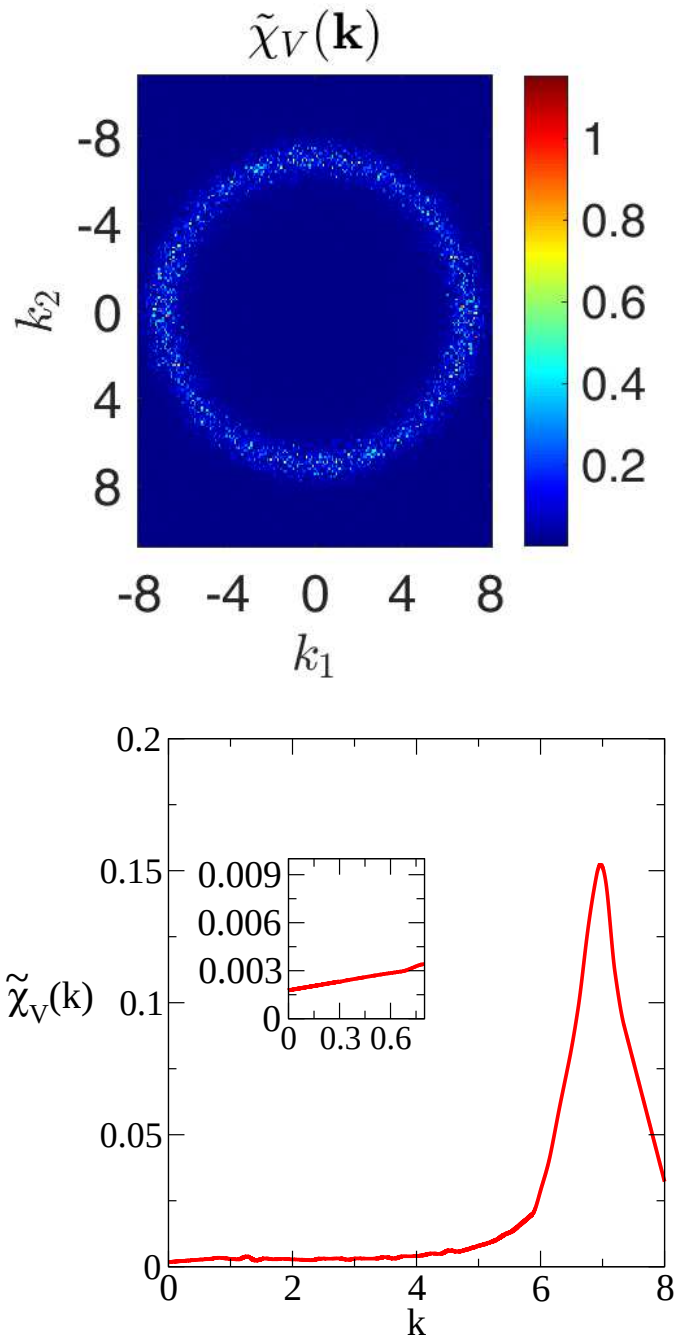

Figure 7. Top panel: Scattering pattern as obtained from the spectral density $\tilde{\chi}_V(\mathbf{k})$ associated with the thresholded version of the Turing image shown in Fig. 6. Bottom panel: Angular-averaged spectral density, $\tilde{\chi}_V(k)$, obtained from the 2D scattering pattern shown in the top panel. The unit of distance used in both spectral plots is the mean chord length of the "yellow" phase [49].

where

$$F(r;K) = c_B(d)\left(\frac{1}{2\pi Kr}\right)^{d/2} K^d J_{d/2}(Kr). \tag{51}$$

Using the results of Appendix A, we can expand the aforementioned putative autocovariance functions about $r = 0$ to yield

$$f_A(\mathbf{r}) = 1 - C_A(d)r^2 + \mathcal{O}(r^4) \tag{52}$$

and

$$f_B(\mathbf{r}) = 1 - C_B(d)r^2 + \mathcal{O}(r^4), \tag{53}$$

where $C_A(d)$ and $C_B(d)$ are positive d-dimensional constants. It immediately follows the autocovariance functions (49) and (50) cannot be realizable by two-phase media since such systems would have a vanishing specific surface s, i.e., the small-r expansion of a valid autocovariance function must be nonanalytic at the origin such that the slope is strictly negative [cf. (2.2.2]. This strongly suggests that scattering patterns in which power is concentrated within some concentric ring of the origin cannot be derived from a two-phase medium. Indeed, any function that is analytic at the origin cannot be an autocovariance function that corresponds to a two-phase medium.

4.3. General Considerations

A general formalism has been proposed that enables the functional form of a realizable autocovariance function to be expressed by a set of chosen realizable basis functions [68]. For our limited purposes in this paper, we will make use of only some of these results. It is known that convex combinations of a set of realizable scaled autocovariance functions $f_1(\mathbf{r}), f_2(\mathbf{r}), \cdots, f_m(\mathbf{r})$ is itself a realizable autocovariance function $f(\mathbf{r})$ [68], i.e.,

$$f(\mathbf{r}) = \sum_{i=1}^{m} \alpha_i f_i(\mathbf{r}), \tag{54}$$

where $0 \le \alpha_i \le 1$ $(i = 1, 2, \ldots, m)$ such that $\sum_{i=1}^{m} \alpha_i = 1$.

In what follows, we focus on basis functions that could correspond to statistically homogeneous and isotropic two-phase media. A simple choice is the radial exponential function:

$$f_1(\mathbf{r}) = \exp(-r/a), \tag{55}$$

which is itself a realizable autocovariance function for all positive and finite a [68]. For reasons discussed at the beginning of this section, the monotonicity of f_1 precludes it from ever corresponding to a hyperuniform two-phase system. It has been shown that a linear combination of f_1 and the basis function

$$f_2(\mathbf{r}) = \exp(-r/b)\cos(qr + \theta) \tag{56}$$

may be realizable for some parameters, but whether such a linear combination can ever correspond to a disordered hyperuniform two-phase system has heretofore not been studied. Here b can be thought of as a characteristic correlation length and q determines the characteristic wavelength associated with the oscillations.

Therefore, we explore here whether a disordered hyperuniform two-phase can have an autocovariance function of the form

$$f(\mathbf{r}) = \alpha_1 \exp(-r/a) + \alpha_2 \exp(-r/b)\cos(qr + \theta), \tag{57}$$

where $\alpha_1 + \alpha_2 = 1$. For simplicity, we examine two special cases. First, we consider the instance in which $\alpha_1 = 0$, $\alpha_2 = 1$ and $\theta = 0$, i.e.,

$$f(\mathbf{r}) = \exp(-r/b)\cos(qr). \tag{58}$$

Notice that the specific surface corresponding to (58) is given by $s = \beta(d)/(b\phi_1\phi_2)$, where $\beta(d)$ is the d-dimensional constant specified in (16). The hyperuniformity sum rule (44) provides conditions on the parameters b and q, which will depend on the dimension. For example, for $d = 1$, we immediately conclude that (58) can never correspond to a hyperuniform medium because (44) cannot be satisfied. On the other hand, for $d = 2$ and $d = 3$, hyperuniformity requires that $(qb)^2 = 1$ and $3(qb)^2 = 1$, respectively, implying that the autocovariance function for a hyperuniform system in a particular dimension generally does not correspond to a hyperuniform system in another dimension. Moreover, these are only necessary conditions on the parameters b and q for the existence of a hyperuniform two-phase medium and one must still check whether the known realizability conditions for two-phase media (described Sec. 2.2.2) are satisfied. As it turns out, all of these realizability conditions are satisfied, including the nonnegativity of the spectral density [cf. 17]. Under these hyperuniform restrictions, the small-k behavior of the spectral density $\tilde{f}(\mathbf{k}) \equiv \tilde{\chi}_v(\mathbf{k})/(\phi_1\phi_2)$ associated with (58) for $d = 2$ and $d = 3$ are given respectively by

$$\frac{\tilde{f}(\mathbf{k})}{b^2} = \frac{3}{4\pi}(kb)^2 - \frac{35}{128\pi}(kb)^6 + \frac{693}{8192\pi}(kb)^{10} + \mathcal{O}(k^{14}), \quad [(qb)^2 = 1] \tag{59}$$

and

$$\frac{\tilde{f}(\mathbf{k})}{b^3} = \frac{27}{4\pi}(kb)^2 - \frac{243}{32\pi}(kb)^4 + \frac{3645}{512\pi}(kb)^8 - \frac{6561}{1024\pi}(kb)^{10} + \mathcal{O}(k^{14}), \quad [3(qb)^2 = 1], \tag{60}$$

where we have made use of the small-argument asymptotic expansion of the Bessel function $J_\nu(x)$ given in Appendix A. Notice also that the hyperuniformity constraint prohibits multiple powers of four in the two-dimensional expansion (59) and multiple powers of six in the three-dimensional expansion (60). In the opposite asymptotic large-k limit, we respectively have for $d = 2$ and $d = 3$

$$\frac{\tilde{f}(\mathbf{k})}{b^2} \sim \frac{2\pi}{(kb)^3}, \qquad k \to \infty \tag{61}$$

and

$$\frac{\tilde{f}(\mathbf{k})}{b^3} \sim \frac{8\pi}{(kb)^4}, \qquad k \to \infty. \tag{62}$$

These results are consistent with the general asymptotic result (18).

Figure 8 shows the autocovariance function and spectral density for a selected set of hyperuniform parameters (b, q) in both two and three dimensions. Not surprisingly, the spectral densities associated with autocovariance functional form (58) differ across dimensions. To verify that there are indeed disordered hyperuniform two-phase media that correspond to these autocovariance, well-established "construction" (reconstruction) optimization techniques devised by Yeong and Torquato [49, 85, 68] are employed. Such procedures utilize simulated-annealing methods that begin with a random initial guess for a digitized two-phase system (hypercubic fundamental simulation box that is tessellated into finer hypercubic cells) satisfying a prescribed volume fraction. The fictitious energy is a sum of squared differences between a target correlation function (or corresponding spectral function) and the correlation function

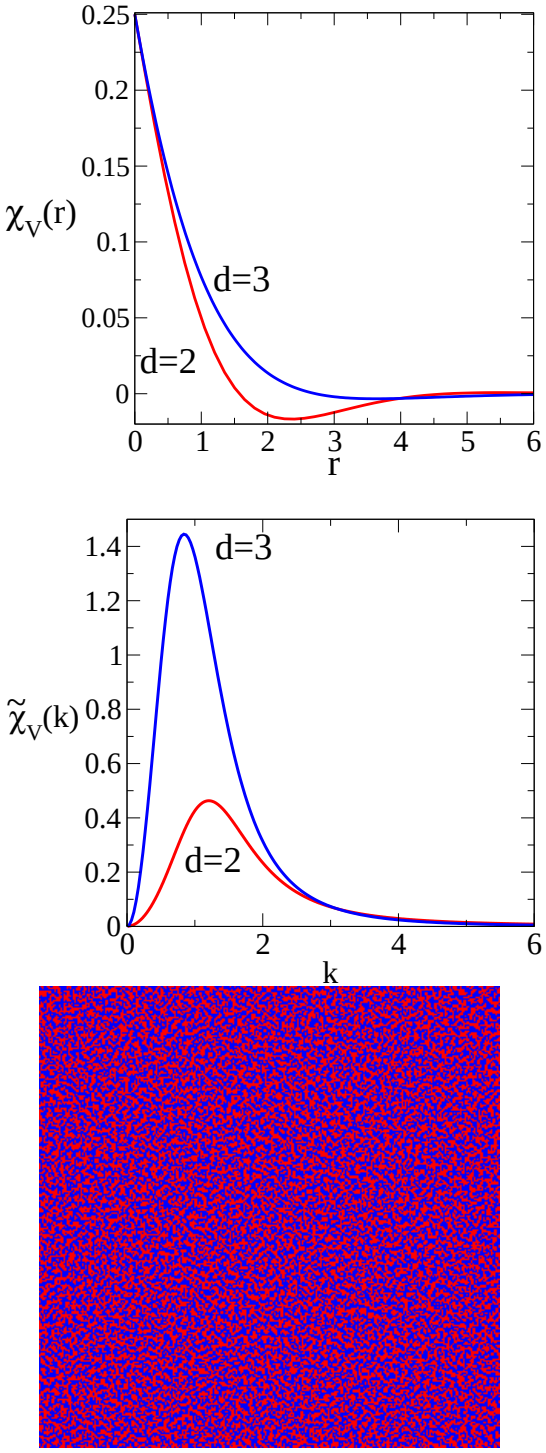

Figure 8. Top panel: Hyperuniform autocovariance function $\chi_V(\mathbf{r})$ given by (58) with $\phi_1 = \phi_2 = 1/2$ in two dimensions where $b = 1$, $q = 1$ and in three dimensions where $b = 1$ and $q = 1/\sqrt{3}$. Middle panel: Corresponding hyperuniform spectral density $\tilde{\chi}_V(\mathbf{k})$ in two and three dimensions. Bottom panel: A realization of a disordered hyperuniform two-phase system that corresponds to (58) in two dimensions with these parameters, as obtained using reconstruction techniques [49, 85, 68]. The final "energy" is smaller than 10^{-9}, indicating that the targeted function is achieved to very high accuracy.

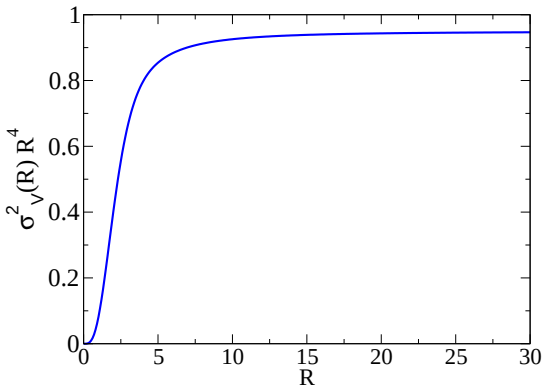

Figure 9. Volume-fraction variance $\sigma_V^2(R)$ (multiplied by R^4) as a function of the window radius using (58) with $\phi_1 = \phi_2 = 1/2$ in three dimensions where $b = 1$, $q = 1/\sqrt{3}$. The fact that this scaled variance asymptotes to a constant value ($243/256 = 0.94921875\ldots$) for large R implies that this three-dimensional hyperuniform system has a variance that decays like R^{-4}, which is consistent with the analytical formula (63).

(or corresponding spectral function) of the simulated structure at any point along the evolution process to the global energy minimum (ground state) as the fictitious temperature tends to zero. Here we target hyperuniform spectral densities associated with (58). The bottom panel of Fig. 8 shows a final construction in the case of two dimensions that corresponds to (58) with extremely high numerical accuracy for a selected set of parameters. Apparently, the known realizability conditions on the function (58) are sufficient to ensure that it corresponds to a two-phase medium in two dimensions. It is noteworthy that it becomes easier to ensure realizability of a hypothesized autocovariance function of specific functional form as the space dimension increases for exactly the same reasons identified for point-configuration realizability [51]. Figure 9 shows the volume-fraction variance $\sigma_v^2(R)$ as a function of the window radius R, as obtained analytically from (29), in the case of three dimensions for a selected set of parameters. We can analytically show that this specific three-dimensional volume-fraction variance has the following asymptotic scaling:

$$\sigma_v^2(R) \sim \frac{243}{256}\frac{1}{R^4} \qquad (R \to \infty). \tag{63}$$

As a second example, we consider the function (57) in which $\alpha_1 = 1/2$, $\alpha_2 = 1/2$ and $\theta = 0$, i.e.,

$$f(\mathbf{r}) = \frac{1}{2}\exp(-r/a) + \frac{1}{2}\exp(-r/b)\cos(qr), \tag{64}$$

which provides greater degrees of freedom to achieve hyperuniformity relative to the form (58). Here a and b are taken to be positive and thus characteristic length scales. The specific surface corresponding to (64) is given by $s = (a+b)\beta(d)/(2ab\,\phi_1\phi_2)$, where $\beta(d)$ is the d-dimensional constant specified in (16). For $d = 1$, we find that (64) can never correspond to a hyperuniform medium because (44) cannot be satisfied, which also was the case for the function (58). This indicates that the hyperuniformity condition is more difficult to achieve in one dimension than in higher dimensions. For

$d = 2$ and $d = 3$, the hyperuniformity sum rule requires that

$$a = \frac{b((qb)^2 - 1)^{1/2}}{(qb)^2 + 1} \tag{65}$$

and

$$a = \frac{b(3(qb)^2 - 1)^{1/3}}{(qb)^2 + 1} \tag{66}$$

respectively. Even though these conditions ensure hyperuniformity in these dimensions, they are not sufficient to guarantee the nonnegativity of the spectral density [cf. 17] for all k because the leading term in the series expansion of $\tilde{f}(\mathbf{k})$ about $k = 0$ is generally quadratic in k but may have a negative coefficient. For example, for $d = 2$, to ensure positivity of the quadratic term, qb must satisfy the following inequalities:

$$1 < qb \leq \frac{1}{2}(\sqrt{6} + \sqrt{2}). \tag{67}$$

If qb is equal to the upper bound in (67), the quadratic term vanishes identically such that the leading term in the expansion of $\tilde{f}(\mathbf{k})$ about $k = 0$ is now quartic in k, which is to be contrasted with the hyperuniform spectral density associated with (58) that goes to zero quadratically in k in the limit $k \to 0$. Under the aforementioned restrictions on the parameters a, b and q, all of the known realizability conditions described in Sec. 2.2.2 are satisfied. Figure 10 shows both the autocovariance function and spectral density for a set of hyperuniform parameters in two dimensions. The bottom panel of Fig. 10 shows a realization obtained by the construction procedure [49, 85, 68] that corresponds to (64) in two dimensions with extremely high numerical accuracy for a selected set of parameters.

5. Conclusions and Discussion

For two-phase media in d-dimensional Euclidean space $\mathbb{R}^d$ in which one of the phases is a packing of spheres, we presented explicit exact expressions for the autocovariance function and associated spectral density as well as upper bounds on the volume-fraction variance in terms of the number variance for any window radius R. We used these results to determine the necessary and sufficient conditions for a sphere packing to be stealthy and hyperuniform as well as to establish rigorously the requirements for a packing comprised of spheres of different sizes to be multihyperuniform. We then considered hyperuniformity for general two-phase media in $\mathbb{R}^d$ outside the class consisting of sphere packings. We applied realizability conditions for an autocovariance function and its associated spectral density of a two-phase medium and incorporated hyperuniformity as a constraint in order to derive new conditions. We showed that some functional forms can immediately be eliminated from consideration and identified other forms that are allowable. Contact was made with well-known two-phase microstructural models (e.g., overlapping spheres and checkerboards) as well as irregular phase-separation and Turing-type patterns. We ascertained a family of autocovariance functions that are realizable by disordered hyperuniform two-phase media in arbitrary space dimensions. Realizations of disordered hyperuniform two-phase media with targeted spectral densities were explicitly constructed. These studies elucidate the nature of hyperuniformity in the context of heterogeneous materials.

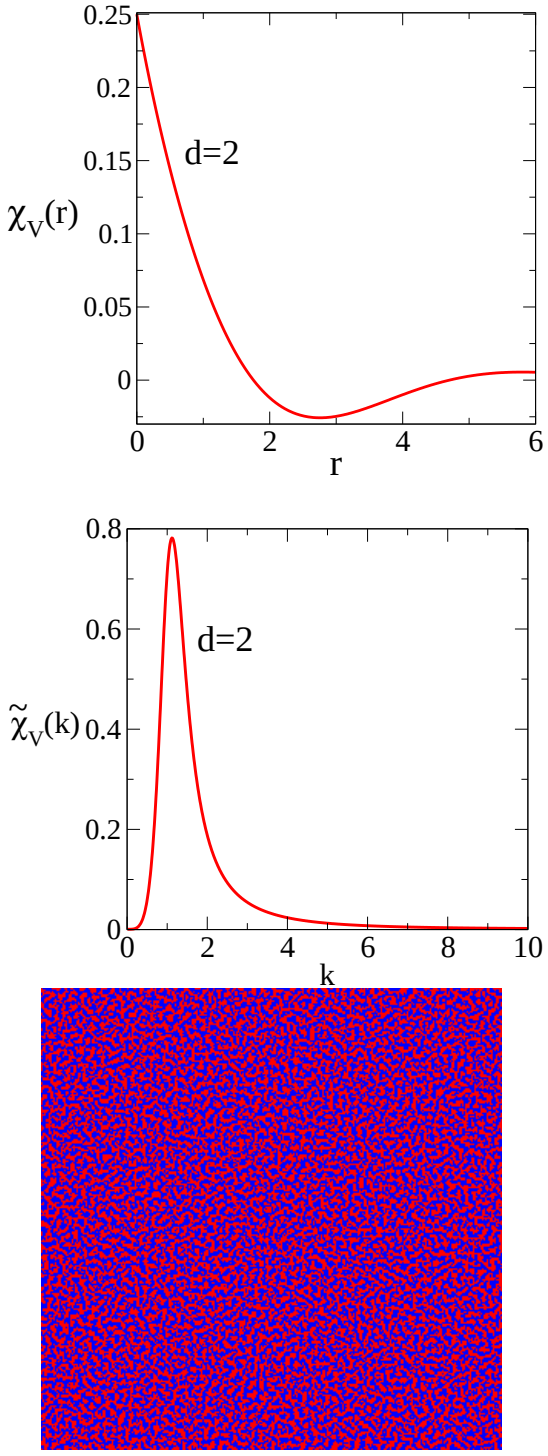

Figure 10. Top panel: Hyperuniform autocovariance function $\chi_V(\mathbf{r})$ given by (64) in two dimensions with $a = (1+\sqrt{3})^{3/2}/(\sqrt{2}(3+\sqrt{3})) = 0.67479019\ldots$ $b = (\sqrt{6}+\sqrt{2})/2 = 1.9318516\ldots$, $q = 1$ and $\phi_1 = \phi_2 = 1/2$. Middle panel: Corresponding hyperuniform spectral density $\tilde{\chi}_V(\mathbf{k})$ in two dimensions. Bottom panel: A realization of a disordered hyperuniform two-phase system that corresponds to (64) in two dimensions with these parameters, as obtained using reconstruction techniques [49, 85, 68]. The final "energy" is smaller than 10^{-9}, indicating that the targeted function is achieved to very high accuracy.

In a subsequent work, we will explore more fully the explicit construction of disordered hyperuniform two-phase media and characterize their higher-order statistics (beyond the two-point autocovariance function) as well as host of other microstructural descriptors that are well-known in homogenization theory [49]. A particularly important goal of such studies will be to develop a deeper understanding of the effect of space dimensionality on the microstructural descriptors, including the relevance of the "decorrelation principle" as the space dimension is increased [51].

A fruitful direction for future research would be the study and determination of the effective physical properties of disordered hyperuniform two-phase systems. There is already evidence demonstrating that disordered hyperuniform cellular network structures possess novel photonic properties [34, 35, 36]. However, the investigation of the bulk properties of general disordered hyperuniform two-phase materials and their technological relevance is essentially uncharted territory, and its exploration may offer great promise for novel materials by design.

Very recently, the hyperuniformity concept was generalized to spin systems and shown to exist as disordered spin ground states [86]. The implications and significance of the existence of such disordered spin systems warrants further study, including whether their bulk physical properties, like their many-particle system counterparts, are singularly remarkable, and can be experimentally realized. Finally, we note that the notion of hyperuniformity has recently been generalized to include surface-area fluctuations in two-phase media as well as fluctuations associated with random scalar and vector fields [72]. Now that we know what to look for, different varieties of disordered hyperuniform systems seem to be arising in surprising places and contexts, and hence offer both intriguing fundamental and applied research challenges and questions for the future.

Appendix A. Fourier Transformation in d Dimensions

We employ the following definition of the Fourier transform of some scalar function $f(\mathbf{r})$ that depends on the vector $\mathbf{r}$ in $\mathbb{R}^d$:

$$\tilde{f}(\mathbf{k}) = \int_{\mathbb{R}^d} f(\mathbf{r}) \exp\left[-i(\mathbf{k}\cdot\mathbf{r})\right] d\mathbf{r}, \tag{A.1}$$

where $\mathbf{k}$ is a wave vector. When it is well-defined, the corresponding inverse Fourier transform is given by

$$f(\mathbf{r}) = \left(\frac{1}{2\pi}\right)^d \int_{\mathbb{R}^d} \tilde{f}(\mathbf{k}) \exp\left[i(\mathbf{k}\cdot\mathbf{r})\right] d\mathbf{k}. \tag{A.2}$$

If f is a radial function, i.e., f depends only on the modulus $r = |\mathbf{r}|$ of the vector $\mathbf{r}$, then its Fourier transform is given by

$$\tilde{f}(k) = (2\pi)^{\frac{d}{2}} \int_0^\infty r^{d-1} f(r) \frac{J_{(d/2)-1}(kr)}{(kr)^{(d/2)-1}}\, dr, \tag{A.3}$$

where $k = |\mathbf{k}|$ is wavenumber or modulus of the wave vector $\mathbf{k}$ and $J_\nu(x)$ is the Bessel function of order ν. The inverse transform of $\tilde{f}(k)$ is given by

$$f(r) = \frac{1}{(2\pi)^{\frac{d}{2}}} \int_0^\infty k^{d-1} \tilde{f}(k) \frac{J_{(d/2)-1}(kr)}{(kr)^{(d/2)-1}} dk. \tag{A.4}$$

We recall the first several terms in the series expansion of $J_\nu(x)$ about $x = 0$:

$$J_\nu(x) = \frac{(x/2)^\nu}{\Gamma(\nu+1)} - \frac{(x/2)^{\nu+2}}{\Gamma(\nu+2)} + \frac{(x/2)^{\nu+4}}{2\Gamma(\nu+3)} - \frac{(x/2)^{\nu+6}}{6\Gamma(\nu+4)} + \mathcal{O}(x^{\nu+8}), \tag{A.5}$$

which we apply in Sec. 4.

Appendix B. Packings of Spheres with a Size Distribution and Multihyperuniformity

Both the autocovariance and associated spectral density for packings of hard spheres with a continuous or discrete size distribution at overall number density ρ have been derived [49, 78]. We collect these results here and apply them to establish rigorously the requirements for multihyperuniformity [28].

In the case of a continuous distribution in radius $\mathcal{R}$ characterized by a probability density function $f(\mathcal{R})$ that normalizes to unity,

$$\int_0^\infty f(\mathcal{R}) d\mathcal{R} = 1, \tag{B.1}$$

the packing fraction and the autocovariance function are given respectively by [78, 49]

$$\phi = \rho \int_0^\infty f(\mathcal{R}) v_1(R) d\mathcal{R} \tag{B.2}$$

and

$$\begin{aligned}\chi_{_V}(\mathbf{r}) = \rho \int_0^\infty f(\mathcal{R}) v_2^{int}(r;\mathcal{R}) d\mathcal{R} \\ + \rho^2 \int_0^\infty d\mathcal{R}_1 \int_0^\infty d\mathcal{R}_2 f(\mathcal{R}_1) f(\mathcal{R}_2)\, m(r;\mathcal{R}_1) \otimes m(r;\mathcal{R}_2) \otimes h(\mathbf{r};\mathcal{R}_1,\mathcal{R}_2),\end{aligned} \tag{B.3}$$

where $h(\mathbf{r};\mathcal{R}_1,\mathcal{R}_2)$ is the appropriate generalization of the total correlation function for the centers of two spheres of radii $\mathcal{R}_1$ and $\mathcal{R}_2$ separated by a distance r. Fourier transformation of (B.3) gives the corresponding spectral density

$$\begin{aligned}\tilde{\chi}_{_V}(\mathbf{k}) = \rho \int_0^\infty f(\mathcal{R}) \tilde{m}^2(k;\mathcal{R}) d\mathcal{R} \\ + \rho^2 \int_0^\infty d\mathcal{R}_1 \int_0^\infty d\mathcal{R}_2 f(\mathcal{R}_1) f(\mathcal{R}_2)\, \tilde{m}(k;\mathcal{R}_1) \tilde{m}(k;\mathcal{R}_2) \tilde{h}(\mathbf{k};\mathcal{R}_1,\mathcal{R}_2).\end{aligned} \tag{B.4}$$

One can obtain corresponding results for spheres with M different radii $a_1, a_2, \ldots, a_M$ from the continuous case by letting

$$f(R) = \sum_{i=1}^M \frac{\rho_i}{\rho} \delta(\mathcal{R} - a_i), \tag{B.5}$$

where ρ_i is the number density of type-i particles, respectively, and ρ is the *total number density*. Substitution of (B.5) into (B.2), (B.3) and (B.4) yields the corresponding packing fraction, autocovariance function and spectral density, respectively, as

$$\phi = \sum_{i=1}^M \rho_i v_1(a_i), \tag{B.6}$$

$$\chi_V(\mathbf{r}) = \sum_{i=1}^{M} \rho_i v_2^{int}(r;a_i) + \sum_{i=1}^{M}\sum_{j=1}^{M} \rho_i\rho_j\, m(r;a_i) \otimes m(r;a_j) \otimes h(\mathbf{r};a_i,a_j) \quad \text{(B.7)}$$

and

$$\tilde{\chi}_V(\mathbf{k}) = \sum_{i=1}^{M} \rho_i \tilde{m}^2(k;a_i) S(\mathbf{k};a_i) + \sum_{i\neq j}^{M} \rho_i\rho_j\, \tilde{m}(k;a_i)\tilde{m}(k;a_j)\tilde{h}(\mathbf{k};a_i,a_j), \quad \text{(B.8)}$$

where

$$S(\mathbf{k};a_i) \equiv 1 + \rho_i \tilde{h}(\mathbf{k};a_i,a_i) \quad \text{(B.9)}$$

is the structure factor for type-i particles. It immediately follows that the spectral density at the origin is given by

$$\begin{aligned}\tilde{\chi}_V(0) = &\sum_{i=1}^{M} \rho_i v_1^2(a_i) S(0;a_i) \\ &+ \sum_{i\neq j}^{M} \rho_i\rho_j\, v_1(a_i) v_1(a_j) \tilde{h}(0;a_i,a_j). \end{aligned} \quad \text{(B.10)}$$

We now prove that when each subpacking associated with each component is hyperuniform, i.e., the first term on the right side of (B.10) is zero, the second term must also be identically zero (sum of cross terms vanish), leading to the hyperuniformity of the entire packing, i.e., $\tilde{\chi}_V(0) = 0$. Such a polydisperse packing has been called multihyperuniform [28].

We begin the proof by considering the spectral density $\tilde{\chi}_V(\mathbf{k})$ for a general, very large but finite-sized two-phase heterogeneous system that is contained within hypercubic fundamental cell in $\mathbb{R}^d$ of side length L and volume $V = L^d$ subjected to periodic boundary conditions, which is given by [67]:

$$\tilde{\chi}_V(\mathbf{k}) = \frac{|\tilde{\mathcal{J}}(\mathbf{k})|^2}{V}, \qquad \mathbf{k} \neq \mathbf{0}, \quad \text{(B.11)}$$

where $\tilde{\mathcal{J}}(\mathbf{k})$ is the discrete Fourier transform of phase indicator function minus the phase volume fraction, which generally is a complex number for any $\mathbf{k} \neq \mathbf{0}$. Ultimately, we take the thermodynamic limit to make contact with (B.10). Consider the two-phase system to be a finite packing of N spheres consisting of M components. Let $\mathbf{r}_1^{(i)}, \ldots, \mathbf{r}_{N_i}^{(i)}$ denote the positions of type-i spheres, where N_i is the total number of spheres of radius a_i and $i = 1, 2, \ldots, M$ such that $N = \sum_{i=1}^{M} N_i$. The discrete Fourier representation of the "scattering amplitude" $\tilde{\mathcal{J}}(\mathbf{k})$ for such a multicomponent packing was given in Ref. [73], which can be recast as follows:

$$\tilde{\mathcal{J}}(\mathbf{k}) = \sum_{i=1}^{M} \tilde{m}(k;a_i) f(\mathbf{k};a_i), \quad \text{(B.12)}$$

where

$$f(\mathbf{k};a_i) = \sum_{n=1}^{N_i} \exp(i\mathbf{k}\cdot\mathbf{r}_n^{(i)}), \quad \text{(B.13)}$$

and the product $\tilde{m}(k;a_i)f(\mathbf{k};a_i)$ represents the scattering amplitude for the ith component (subpacking). Substitution of (B.12) into (B.11) yields

$$\tilde{\chi}_V(\mathbf{k}) = \sum_{i=1}^{M} \rho_i \tilde{m}^2(k;a_i)\mathcal{S}(\mathbf{k};a_i) + \sum_{i\neq j}^{M} \rho_i\rho_j\, \tilde{m}(k;a_i)\tilde{m}(k;a_j)\mathcal{H}(\mathbf{k};a_i,a_j), \quad \text{(B.14)}$$

where

$$\mathcal{S}(\mathbf{k};a_i)=\frac{|f(\mathbf{k};a_i)|^2}{N_i} \tag{B.15}$$

is the discrete structure factor for the ith subpacking and

$$\mathcal{H}(\mathbf{k};a_i,a_j)=\frac{f(\mathbf{k};a_i)f(\mathbf{k};a_j)\,V}{N_iN_j}. \tag{B.16}$$

The similarity between this discrete representation of the spectral density of a multicomponent packing and the continuous version (B.8) is readily apparent.

The chosen hypercubic fundamental cell restricts the wave vectors to take discrete values, which are defined by the vectors that span the reciprocal hypercubic lattice, i.e., $\mathbf{k}=(2\pi n_1/L,2\pi n_2/L,\cdots,2\pi n_d/L)$, where n_i $(i=1,2,\ldots,d)$ are the integers. Thus, the smallest positive wave vectors have magnitude $k_{min}=2\pi/L$. Now we constrain the scattering amplitude for each component to be zero at $|\mathbf{k}|=k_{min}$, which from (B.12) implies that $\tilde{\mathcal{J}}(|\mathbf{k}|=k_{min})=0$ and hence $\tilde{\chi}_V(|\mathbf{k}|=k_{min})=0$. This in turn means that the second sum (B.14) involving the cross terms must vanish at $|\mathbf{k}|=k_{min}$. To complete the proof, we must consider the thermodynamic limit because the ensemble-average relation (B.10) applies under this condition. Assuming ergodic media, the zero-wave-vector behavior of the spectral density defined by (B.10) can be extracted from the discrete spectrum (B.11) in the thermodynamic limit, i.e.,

$$\tilde{\chi}_V(\mathbf{0})\equiv\lim_{N,V\to\infty}\tilde{\chi}_V(|\mathbf{k}|=k_{min}). \tag{B.17}$$

The limit here is taken at constant number density $\rho=N/V$, implying that $k_{min}\to 0$. Under the prescribed conditions mentioned above, we find that $\tilde{\chi}_V(\mathbf{0})=0$, which completes the proof.

Acknowledgments

The author dedicates this article to the honor the memory of Professor George Stell, mentor and colleague, for his seminal research contributions to statistical mechanics. The author thanks Duyu Chen, Jaeuk Kim and Zheng Ma for their careful reading of the manuscript. He is especially grateful to Duyu Chen for his assistance in creating the microstructure-construction figure. This work was supported by the National Science Foundation under Grant No. DMS-1211087.

[1] S. Torquato and F. H. Stillinger. Local density fluctuations, hyperuniform systems, and order metrics. *Phys. Rev. E*, 68:041113, 2003.

[2] B. Widom. Equation of state in the neighborhood of the critical point. *J. Chem. Phys.*, 43:3898–3905, 1965.

[3] L. P. Kadanoff. Scaling laws for ising models near T_c. *Physics*, 2:263–272, 1966.

[4] M. E. Fisher. The theory of equilibrium critical phenomena. *Rep. Prog. Phys.*, 30:615, 1967.

[5] K. G. Wilson and J. Kogut. The renormalization group and the ϵ expansion. *Phys. Rep.*, 12:75–199, 1974.

[6] A. Gabrielli, M. Joyce, and F. Sylos Labini. Glass-like universe: Real-space correlation properties of standard cosmological models. *Phys. Rev. D*, 65:083523, 2002.

[7] C. E. Zachary and S. Torquato. Hyperuniformity in point patterns and two-phase heterogeneous media. *J. Stat. Mech.: Theory & Exp.*, page P12015, 2009.

[8] C. E. Zachary and S. Torquato. Anomalous local coordination, density fluctuations, and void statistics in disordered hyperuniform many-particle ground states. *Phys. Rev. E*, 83:051133, 2011.

[9] S. Torquato, G. Zhang, and F. H. Stillinger. Ensemble Theory for Stealthy Hyperuniform Disordered Ground States. *Phys. Rev. X*, 5:021020, 2015.

[10] J. L. Lebowitz. Charge fluctuations in Coulomb systems. *Phys. Rev. A*, 27:1491–1494, 1983.
[11] A. Donev, F. H. Stillinger, and S. Torquato. Unexpected density fluctuations in disordered jammed hard-sphere packings. *Phys. Rev. Lett.*, 95:090604, 2005.
[12] O. U. Uche, F. H. Stillinger, and S. Torquato. Constraints on collective density variables: Two dimensions. *Phys. Rev. E*, 70:046122, 2004.
[13] R. D. Batten, F. H. Stillinger, and S. Torquato. Classical disordered ground states: Super-ideal gases, and stealth and equi-luminous materials. *J. Appl. Phys.*, 104:033504, 2008.
[14] M. Florescu, S. Torquato, and P. J. Steinhardt. Designer disordered materials with large complete photonic band gaps. *Proc. Nat. Acad. Sci.*, 106:20658–20663, 2009.
[15] C. E. Zachary, Y. Jiao, and S. Torquato. Hyperuniform long-range correlations are a signature of disordered jammed hard-particle packings. *Phys. Rev. Lett.*, 106:178001, 2011.
[16] Y. Jiao and S. Torquato. Maximally random jammed packings of Platonic solids: Hyperuniform long-range correlations and isostaticity. *Phys. Rev. E*, 84:041309, 2011.
[17] D. Chen, Y. Jiao, and S. Torquato. Equilibrium phase behavior and maximally random jammed state of truncated tetrahedra. *J. Phys. Chem. B*, 118:7981–7992, 2014.
[18] L. Berthier, P. Chaudhuri, C. Coulais, O. Dauchot, and P. Sollich. Suppressed compressibility at large scale in jammed packings of size-disperse spheres. *Phys. Rev. Lett.*, 106:120601, 2011.
[19] R. Kurita and E. R. Weeks. Incompressibility of polydisperse random-close-packed colloidal particles. *Phys. Rev. E*, 84:030401, 2011.
[20] R. Dreyfus, Y. Xu, T. Still, L. A. Hough, A. G. Yodh, and S. Torquato. Diagnosing hyperuniformity in two-dimensional, disordered, jammed packings of soft spheres. *Phys. Rev. E*, 91:012302, 2015.
[21] I. Lesanovsky and J. P. Garrahan. Out-of-equilibrium structures in strongly interacting Rydberg gases with dissipation. *Phys. Rev. A*, 90:011603, 2014.
[22] R. L. Jack, I. R. Thompson, and P. Sollich. Hyperuniformity and phase separation in biased ensembles of trajectories for diffusive systems. *Phys. Rev. Lett.*, 114:060601, 2015.
[23] D. Hexner and D. Levine. Hyperuniformity of critical absorbing states. *Phys. Rev. Lett.*, 114:110602, 2015.
[24] J. H. Weijs, R. Jeanneret, R. Dreyfus, and D. Bartolo. Emergent hyperuniformity in periodically driven emulsions. *Phys. Rev. Lett.*, 115:108301, 2015.
[25] E. Tjhung and L. Berthier. Hyperuniform density fluctuations and diverging dynamic correlations in periodically driven colloidal suspensions. *Phys. Rev. Lett.*, 114:148301, 2015.
[26] R. Dickman and S. D. da Cunha. Particle-density fluctuations and universality in the conserved stochastic sandpile. *Phys. Rev. E*, 92:020104, 2015.
[27] K. J. Schrenk and D. Frenkel. Communication: Evidence for non-ergodicity in quiescent states of periodically sheared suspensions. *J. Chem. Phys.*, 143, 2015.
[28] Y. Jiao, T. Lau, H. Hatzikirou, M. Meyer-Hermann, J. C. Corbo, and S. Torquato. Avian photoreceptor patterns represent a disordered hyperuniform solution to a multiscale packing problem. *Phys. Rev. E*, 89:022721, 2014.
[29] L. M. Burcaw, E. Fieremans, and D. S. Novikov. Mesoscopic structure of neuronal tracts from time-dependent diffusion. *NeuroImage*, 114:18–37, 2015.
[30] S. Torquato, A. Scardicchio, and C. E. Zachary. Point processes in arbitrary dimension from Fermionic gases, random matrix theory, and number theory. *J. Stat. Mech.: Theory Exp.*, page P11019, 2008.
[31] R. P. Feynman and M. Cohen. Energy spectrum of the excitations in liquid helium. *Phys. Rev.*, 102:1189–1204, 1956.
[32] G. Zhang, F. Stillinger, and S. Torquato. Ground states of stealthy hyperuniform potentials: I. Entropically favored configurations. *Phys. Rev. E*, 92:022119, 2015.
[33] G. Zhang, F. Stillinger, and S. Torquato. Ground states of stealthy hyperuniform potentials: II. Stacked-slider phases. *Phys. Rev. E*, 92:022120, 2015.
[34] W. Man, M. Florescu, K. Matsuyama, P. Yadak, G. Nahal, S. Hashemizad, E. Williamson, P. Steinhardt, S. Torquato, and P. Chaikin. Photonic band gap in isotropic hyperuniform disordered solids with low dielectric contrast. *Opt. Express*, 21:19972–19981, 2013.
[35] J. Haberko, N. Muller, and F. Scheffold. Direct laser writing of three dimensional network structures as templates for disordered photonic materials. *Phys. Rev. A*, 88:043822, 2013.
[36] W. Man, M. Florescu, E. P. Williamson, Y. He, S. R. Hashemizad, B. Y. C. Leung, D. R. Liner, S. Torquato, P. M. Chaikin, and P. J. Steinhardt. Isotropic band gaps and freeform waveguides observed in hyperuniform disordered photonic solids. *Proc. Nat. Acad. Sci.*, 110:15886–15891, 2013.
[37] C. De Rosa, F. Auriemma, C. Diletto, R. Di Girolamo, A. Malafronte, P. Morvillo, G. Zito, G. Rusciano, G. Pesce, and A. Sasso. Toward hyperuniform disordered plasmonic

nanostructures for reproducible surface-enhanced Raman spectroscopy. *Phys. Chem. Chem. Phys.*, 17:8061–8069, 2015.

[38] R. Degl'Innocenti, Y. D. Shah, L. Masini, A. Ronzani, A. Pitanti, Y. Ren, D. S. Jessop, A. Tredicucci, H. E. Beere, and D. A. Ritchie. Thz quantum cascade lasers based on a hyperuniform design. *Proc. SPIE*, 9370:93700A–93700A–6, 2015.

[39] G. Zito, G. Rusciano, G. Pesce, A. Malafronte, R. Di Girolamo, G. Ausanio, A. Vecchione, and A. Sasso. Nanoscale engineering of two-dimensional disordered hyperuniform block-copolymer assemblies. *Phys. Rev. E*, 92:050601, 2015.

[40] M. Hejna, P. J. Steinhardt, and S. Torquato. Nearly hyperuniform network models of amorphous silicon. *Phys. Rev. B*, 87:245204, 2013.

[41] R. Xie, G. G. Long, S. J. Weigand, S. C. Moss, T. Carvalho, S. Roorda, M. Hejna, S. Torquato, and P. J Steinhardt. Hyperuniformity in amorphous silicon based on the measurement of the infinite-wavelength limit of the structure factor. *Proc. Nat. Acad. Sci.*, 110:13250–13254, 2013.

[42] É. Marcotte, F. H. Stillinger, and S. Torquato. Nonequilibrium static growing length scales in supercooled liquids on approaching the glass transition. *J. Chem. Phys.*, 138:12A508, 2013.

[43] V. Lubchenko and P. G. Wolynes. Theory of structural glasses and supercooled liquids. *Ann. Rev. Phys. Chem.*, 58:235–266, 2007.

[44] L. Berthier, G. Biroli, J.-P. Bouchaud, W. Kob, K. Miyazaki, and D. R. Reichman. Spontaneous and induced dynamic fluctuations in glass formers. i. general results and dependence on ensemble and dynamics. *J. Chem. Phys.*, 126, 2007.

[45] K. S. Schweizer. Dynamical fluctuation effects in glassy colloidal suspensions. *Current Opinion Coll. Inter. Sc.*, 12:297 – 306, 2007.

[46] S. Karmakar, C. Dasgupta, and S. Sastry. Growing length and time scales in glass-forming liquids. *Proc. Nat. Acad. Sci.*, 106:3675–3679, 2009.

[47] D. Chandler and J. P. Garrahan. Dynamics on the way to forming glass: Bubbles in space-time. *Ann. Rev. Phys. Chem.*, 61:191–217, 2010.

[48] G. M. Hocky, T. E. Markland, and D. R. Reichman. Growing point-to-set length scale correlates with growing relaxation times in model supercooled liquids. *Phys. Rev. Lett.*, 108:225506, 2012.

[49] S. Torquato. *Random Heterogeneous Materials: Microstructure and Macroscopic Properties*. Springer-Verlag, New York, 2002.

[50] M. Sahimi. *Heterogeneous Materials I: Linear Transport and Optical Properties*. Springer-Verlag, New York, 2003.

[51] S. Torquato and F. H. Stillinger. New conjectural lower bounds on the optimal density of sphere packings. *Experimental Math.*, 15:307–331, 2006.

[52] P. Debye and A. M. Bueche. Scattering by an inhomogeneous solid. *J. Appl. Phys.*, 20:518–525, 1949.

[53] P. Debye, H. R. Anderson, and H. Brumberger. Scattering by an inhomogeneous solid. II. The correlation function and its applications. *J. Appl. Phys.*, 28:679–683, 1957.

[54] S. Torquato and G. Stell. Microstructure of two-phase random media: I. The n-point probability functions. *J. Chem. Phys.*, 77:2071–2077, 1982.

[55] S. Torquato and G. Stell. Microstructure of two-phase random media: II. The Mayer–Montroll and Kirkwood–Salsburg hierarchies. *J. Chem. Phys.*, 78:3262–3272, 1983.

[56] S. Torquato. Effective electrical conductivity of two-phase disordered composite media. *J. Appl. Phys.*, 58:3790–3797, 1985.

[57] J. G. Berryman and G. W. Milton. Normalization constraint for variational bounds on fluid permeability. *J. Chem. Phys.*, 83:754–760, 1985.

[58] J. G. Berryman and G. W. Milton. Microgeometry of random composites and porous media. *J. Phys. D: Appl. Phys.*, 21:87–94, 1988.

[59] A. K. Sen and S. Torquato. Effective conductivity of anisotropic two-phase composite media. *Phys. Rev. B*, 39:4504–4515, 1989.

[60] L. V. Gibiansky and S. Torquato. Geometrical-parameter bounds on effective moduli of composites. *J. Mech. Phys. Solids*, 43:1587–1613, 1995.

[61] G. W. Milton. *The Theory of Composites*. Cambridge University Press, Cambridge, England, 2002.

[62] D. C. Pham and S. Torquato. Strong-contrast expansions and approximations for the effective conductivity of isotropic multiphase composites. *J. Appl. Phys.*, 94:6591–6602, 2003.

[63] S. Torquato and D. C. Pham. Optimal bounds on the trapping constant and permeability of porous media. *Phys. Rev. Lett.*, 92:255505, 2004.

[64] S. Torquato. Exact expression for the effective elastic tensor of disordered composites. *Phys.*

Rev. Lett., 79:681–684, 1997.

[65] M. C. Rechtsman and S. Torquato. Effective dielectric tensor for electromagnetic wave propagation in random media. *J. Appl. Phys.*, 103:084901, 2008.

[66] M. B. Priestley. *Spectral Analysis and Time Series*. Academic Press, New York, 1981.

[67] S. Torquato. Exact conditions on physically realizable correlation functions of random media. *J. Chem. Phys.*, 111:8832–8837, 1999.

[68] Y. Jiao, F. H. Stillinger, and S. Torquato. Modeling heterogeneous materials via two-point correlation functions: Basic principles. *Phys. Rev. E*, 76:031110, 2007.

[69] J. Quintanilla. Necessary and sufficient conditions for the two-point probability function of two-phase random media. *Proc. R. Soc. Lond. A.*, 464:1761–1779, 2008.

[70] R. Lachieze-Rey and I. Molchanov. Regularity conditions in the realisability problem with applications to point processes and random closed sets. *Annals Appl. Prob.*, 25:116–149, 2015.

[71] B. L. Lu and S. Torquato. Local volume fraction fluctuations in heterogeneous media. *J. Chem. Phys.*, 93:3452–3459, 1990.

[72] S. Torquato. Hyperuniformity and its generalizations. *Phys. Rev. E*, in press: arXiv: 1607.08814.

[73] C. E. Zachary, Y. Jiao, and S. Torquato. Hyperuniformity, quasi-long-range correlations, and void-space constraints in maximally random jammed particle packings. I. Polydisperse spheres. *Phys. Rev. E*, 83:051308, 2011.

[74] C. E. Zachary, Y. Jiao, and S. Torquato. Hyperuniformity, quasi-long-range correlations, and void-space constraints in maximally random jammed particle packings. II. Anisotropy in particle shape. *Phys. Rev. E*, 83:051309, 2011.

[75] D. Chen and S. Torquato. Confined disordered strictly jammed binary sphere packings. *Phys. Rev. E*, 92:062207, 2015.

[76] S. Torquato and G. Stell. Microstructure of two-phase random media: V. The n-point matrix probability functions for impenetrable spheres. *J. Chem. Phys.*, 82:980–987, 1985.

[77] S. Torquato. Statistical description of microstructures. *Ann. Rev. Mater. Res.*, 32:77–111, 2002.

[78] B. L. Lu and S. Torquato. General formalism to characterize the microstructure of polydispersed random media. *Phys. Rev. A*, 43:2078–2080, 1991.

[79] S. Torquato and G. Stell. Microstructure of two-phase random media: III. The n-point matrix probability functions for fully penetrable spheres. *J. Chem. Phys.*, 79:1505–1510, 1983.

[80] D. A. Coker, S. Torquato, and J. H. Dunsmuir. Morphology and physical properties of Fontainebleau sandstone via a tomographic analysis. *J. Geophys. Res.*, 101:17497–17506, 1996.

[81] S. Torquato and F. Lado. Characterisation of the microstructure of distributions of rigid rods and discs in a matrix. *J. Phys. A: Math. & Gen.*, 18:141–148, 1985.

[82] J. W. Cahn and J. E. Hilliard. Free energy of a nonuniform system. i. interfacial free energy. *J. Chem. Phys.*, 28:258–267, 1958.

[83] J. Swift and P. C. Hohenberg. Hydrodynamic fluctuations at the convective instability. *Phys. Rev. A*, 15:319–328, 1977.

[84] Pattern formation. `https://en.wikipedia.org/wiki/Pattern_formation`.

[85] C. L. Y. Yeong and S. Torquato. Reconstructing random media. *Phys. Rev. E*, 57:495–506, 1998.

[86] E. Chertkov, R. A. DiStasio, G. Zhang, R. Car, and S. Torquato. Inverse design of disordered stealthy hyperuniform spin chains. *Phys. Rev. B*, 93:064201, 2015.